

# Visible-Light-Driven Photoreactions of $[(\text{bpy})_2\text{Ru}(\text{II})\text{L}]\text{Cl}_2$ in Aqueous Solutions (bpy = Bipyridine, L = 1,2-Bis(4-(4'-methyl)-2,2'-bipyridyl) Ethene)

Haoyu Zhang, Cheruvallil S. Rajesh, and Prabir K. Dutta\*

Department of Chemistry, 120 West 18th Avenue, The Ohio State University, Columbus, Ohio 43210

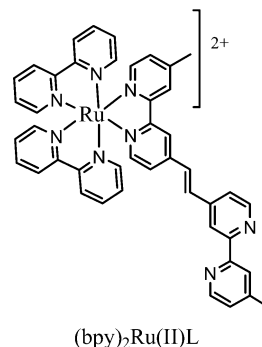
Received: August 13, 2007; In Final Form: November 7, 2007

Visible-light-induced photoreactions of  $[(\text{bpy})_2\text{Ru}(\text{II})\text{L}]\text{Cl}_2$  (bpy = bipyridine, L = *trans*-1,2-bis(4-(4'-methyl)-2,2'-bipyridyl) ethene) in aqueous solution are examined. From pH titrations, it is found that the Ru complex is a stronger base ( $\text{p}K_{\text{a}}^* = 6$ ) in the excited state than in the ground state ( $\text{p}K_{\text{a}} = 4$ ). Photolysis of the  $[(\text{bpy})_2\text{Ru}(\text{II})\text{L}]$  complex in solutions at pH 7 and 12 led to formation of species with increased emission quantum yields,  $\sim 55$  nm blue-shift of the emission maximum to 625 nm, and disappearance of the absorption band at 330 nm, the latter arising from the olefinic bond of the L ligand. No spectral changes are observed in solutions at  $\text{pH} \leq 4$ . With the help of chromatography, mass spectroscopy, Raman spectroscopy, and NMR, photoproducts formed at neutral pH have been analyzed. It is found that the major product is a dimer of  $[(\text{bpy})_2\text{Ru}(\text{II})\text{L}]$ , dimerizing around the double bond. Photoreactions do not occur in the dark or in the aprotic solvent acetonitrile. We propose that a Ru(III) radical intermediate is formed by photoinduced excited-state electron and proton transfer, which initiates the dimerization. The radical intermediate can also undergo photochemical degradative reductions. Below pH 4, the emission quenching is proposed to arise via protonation of the monoprotonated  $[(\text{bpy})_2\text{Ru}(\text{II})\text{LH}]$  followed by electron transfer to the viologen-type moiety created by protonation. The products of photodegradation at  $\text{pH} > 12$  are different from those of pH 7, but the mechanism of the degradation at  $\text{pH} > 12$  was not elucidated.

## I. Introduction

Polypyridine complexes of ruthenium have been studied extensively for applications in energy conversion,<sup>1–5</sup> charge separation,<sup>6–11</sup> luminescence sensing,<sup>12</sup> photocatalysis<sup>13</sup> and as photochemical molecular devices.<sup>14,15</sup> Metal-to-ligand charge transfer (MLCT) states of these complexes play a major role in their photochemical and photophysical processes. The characteristics of the MLCT state can be altered by varying the ligands.<sup>1,16</sup> Ruthenium complexes containing rigid ligands with extended  $\pi$ -conjugation systems tend to have longer excited-state lifetimes as a result of shorter bond displacements in the excited state.<sup>17</sup> Stilbene-like N-heterocyclic compounds represent such a class of ligands,<sup>18,19</sup> and their photochemistry in aqueous solutions has been extensively studied.<sup>19–22</sup> These molecules undergo photoaddition and photoreduction reactions involving radical intermediates, where the corresponding hydrocarbons are unreactive. Transition metal complexes containing stilbene-like ligands have been synthesized, and their photophysical and photochemical properties have been reported.<sup>9h,23–27</sup> Several studies have shown that photoreactions including *trans*–*cis* isomerization occur under UV-light irradiation in organic solvents. However, their photochemical properties in aqueous solutions have not been explored. Another important feature of Ru complexes containing protonable ligands is their acid–base reactions in the excited state.<sup>28–35</sup> Charge localization on the ligand in the MLCT state can lead to pH-dependent luminescence properties.

In this paper, we explore the photoreactions of  $(\text{bpy})_2\text{Ru}(\text{II})\text{L}$  (bpy = 2,2'-bipyridine, L = *trans*-1,2-bis-(4-(4'-methyl)-2,2'-bipyridyl)ethene, structure shown below) in aqueous solutions.



Synthesis of L and the corresponding Ru complexes has been reported by Strouse et al.<sup>17</sup> We report here that the absorption and emission spectra of aqueous solutions of  $[(\text{bpy})_2\text{RuL}]^{2+}$  exhibit significant changes under visible-light irradiation. The photochemistry is pH-dependent and occurred in neutral and basic aqueous solutions. Photoproducts were analyzed by chromatography, spectroscopy, and mass spectrometry. We suggest that a radical intermediate arising from excited-state protonation and electron transfer is involved in the photoreactions and leads to the formation of the dimer of  $[(\text{bpy})_2\text{RuL}]^{2+}$  as the major photoproduct. At  $\text{pH} \leq 4$ , excited-state protonation and electron transfer occur without any new photochemical products.

## II. Experimental Section

**II.1. Materials.** The  $[(\text{bpy})_2\text{Ru}(\text{II})\text{L}](\text{PF}_6)_2$  was synthesized as described elsewhere.<sup>9i,17</sup> The chloride salt  $[(\text{bpy})_2\text{Ru}(\text{II})\text{L}]\text{Cl}_2$  was prepared by treating a solution of the  $\text{PF}_6^-$  salt in acetone with lithium chloride and recovered by filtration. Sodium 1-heptanesulfonate monohydrate was purchased from Sigma-Aldrich.

\* To whom correspondence should be addressed. E-mail: dutta.1@osu.edu. Phone: 614-292-4532. Fax: 614-688-5402.

**II.2. Photolysis.** The light source was a Xenon arc lamp equipped with a water filter and a UV and 430 nm cutoff filter. The power of the radiation incident on the substrate side of the cell was measured by a Coherent 210 power meter and found to be  $\sim 150$  mW/cm<sup>2</sup>. Spectral changes associated with irradiation of samples were monitored with a UV–vis spectrophotometer (Shimadzu, UV-2501PC), and emission spectra were measured using a Spex Fluorolog fluorimeter.

**II.3. Resonance Raman Spectroscopy.** Resonance Raman spectra were obtained on  $\sim 1 \times 10^{-3}$  M samples in CH<sub>3</sub>CN at 298 K. Raman Spectra were taken by a HORIBA-Jobin Yvon HR800 spectrometer with excitation at 488 nm.

**II.4. High-Performance Liquid Chromatography (HPLC).** A Shimadzu series LC-10AT pump LC system and a Rheodyne sample injector with 20  $\mu$ L and 100  $\mu$ L loops, and a Shimadzu SPD-M10a diode array UV–vis detector were used. Separation was achieved by means of reversed-phase ion-pair chromatography.<sup>36</sup> Analytical separations were carried out on a Symmetryshield PR18 reversed-phase column (150 mm  $\times$  4.6 mm, 100  $\text{Å}$ , 5  $\mu$ m, Waters Corporation), and semipreparative work was done on a Sunfire reversed-phase column (250 mm  $\times$  10 mm, 100  $\text{Å}$ , 5  $\mu$ m, Waters Corporation) with detection at variable wavelengths. The mobile phase was comprised of water (solvent A) and methanol (solvent B). Both A and B contained 5 mM sodium 1-heptanesulfonate as the ion-pairing agent.

For analytical assays, the flow rate was 1.0 mL/min, for semipreparative work, 4 mL/min. Aqueous solutions of the metal complexes containing the ion-pairing agent were then passed through the column. The desired components were then eluted with aqueous methanol (the larger the percent of methanol in the mixture, the more facile the elution). The chloride salts of photoproducts were prepared by dissolving the heptanesulfonate salt in water, passing the solution through Dowex 1-X8 anion exchange resin in the chloride form, and evaporating the resulting solution to dryness.

**II.5. Liquid Chromatography Mass Spectrometry (LC–MS).** Experiments were performed on a Micromass LC–Tof II (Micromass, Wythenshawe, U.K.) mass spectrometer equipped with an orthogonal electrospray source (Z-spray) operated in positive ion mode. Sodium iodide was used for mass calibration for a calibration range of  $m/z$  100–2000. Optimal ESI conditions were the following: capillary voltage 3000 V, source temperature 110  $^{\circ}$ C, and a cone voltage of 55 V. The ESI gas was nitrogen. All ions transmitted into the pusher region of the TOF analyzer were scanned over  $m/z$  300–1000 with a 1 s integration time. Data was acquired in continuum mode during the LC run. The liquid chromatographic/autosampler system consisted of a Waters Alliance 2690 separations module (Waters, Milford, MA) and Symmetryshield PR18 reversed-phase column (150 mm  $\times$  4.6 mm, 100  $\text{Å}$ , 5  $\mu$ m, Waters Corporation). The mobile phase was comprised of 30% water and 70% methanol. Both solvents contained 5 mM sodium 1-heptanesulfonate as the ion-pairing agent. The mobile phase flow rate was maintained at 1.0 mL/min and was split postcolumn using a microsplits valve (Upchurch Scientific, Oak Harbor, WA) to  $\sim 20$   $\mu$ L/min for introduction to the ESI source.

**II.6. Electrospray Ionization Mass Spectrometry (ESI–MS).** All experiments were performed on a Micromass ESI–Tof II (Micromass, Wythenshawe, U.K.) mass spectrometer equipped with an orthogonal electrospray source (Z-spray) operated in positive ion mode. Sodium iodide was used for mass calibration for a calibration range of  $m/z$  100–2000. Samples were prepared in a solution containing acidified methanol and infused into the electrospray source at a rate of 5–10 mL min<sup>-1</sup>.

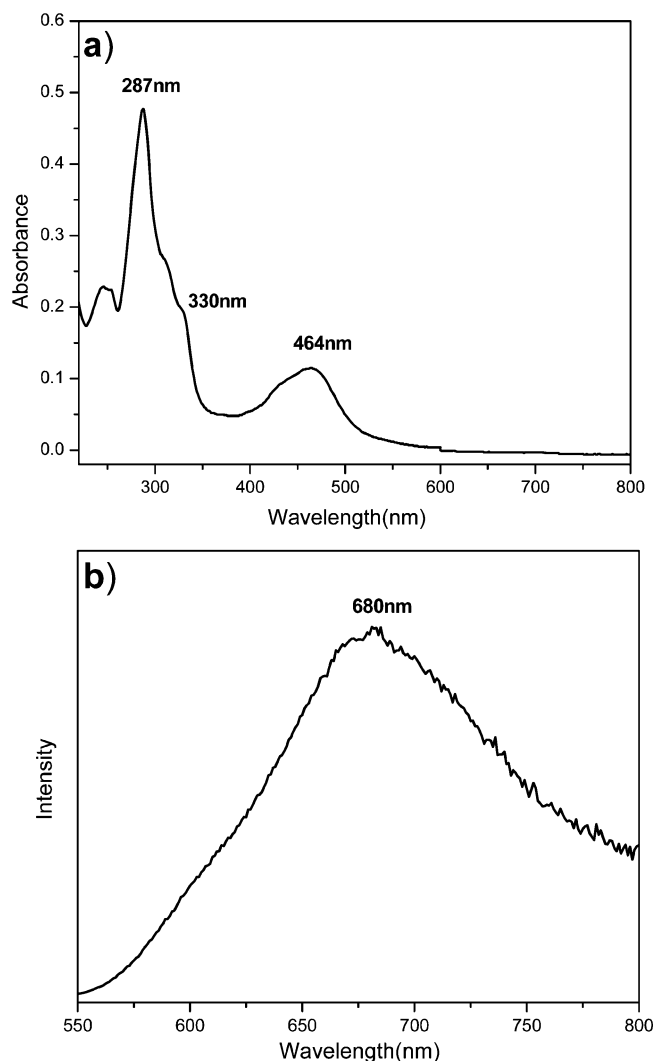


**Figure 1.** (a) Absorption and (b) emission spectra of [(bpy)<sub>2</sub>RuL]<sup>2+</sup>·2Cl<sup>-</sup> ( $1.0 \times 10^{-5}$  M, excitation wavelength is 450 nm) in water (pH = 7.0).

For exact mass measurements, all spectra were combined, smoothed, and centroided, and internal calibration with mass of sodium iodide clusters was used. Optimal ESI conditions were the following: capillary voltage 3000 V, source temperature 110  $^{\circ}$ C, and a cone voltage of 55 V. The ESI gas was nitrogen. Data were acquired in a continuum mode until acceptable averaged data were obtained.

**II.7. Nuclear Magnetic Resonance (NMR) Spectroscopy.** For HPLC-isolated photoproducts, NMR data were acquired at a temperature of 298 K using a Bruker 400 MHz NMR spectrometer.

### III. Results

Figure 1 shows the absorption and emission spectra of [(bpy)<sub>2</sub>RuL]<sup>2+</sup>·2Cl<sup>-</sup> in distilled water. The electronic spectrum consists of well-resolved bands at  $\sim 287$  and  $\sim 330$  nm assigned to intraligand  $\pi$ – $\pi^*$  transitions of bpy and L, respectively, and a band at  $\sim 464$  nm attributed to the MLCT transition. The complex in neutral aqueous solutions has an emission maximum at  $\sim 680$  nm (Figure 1b). Lifetimes were measured in acetonitrile (PF<sub>6</sub><sup>-</sup> salt) and in acidic pH. Biexponential fits were required in CH<sub>3</sub>CN, with lifetimes of 710 (82%) and 256 ns (18%). At pH  $\sim 3.2$ , three lifetimes of 765 (38%), 531 (44%), and 109 ns (18%) were necessary for an adequate fit.

**III.1. Acid–Base Reactions in the Ground and Excited States.** Acid–base equilibria are expected in both ground and

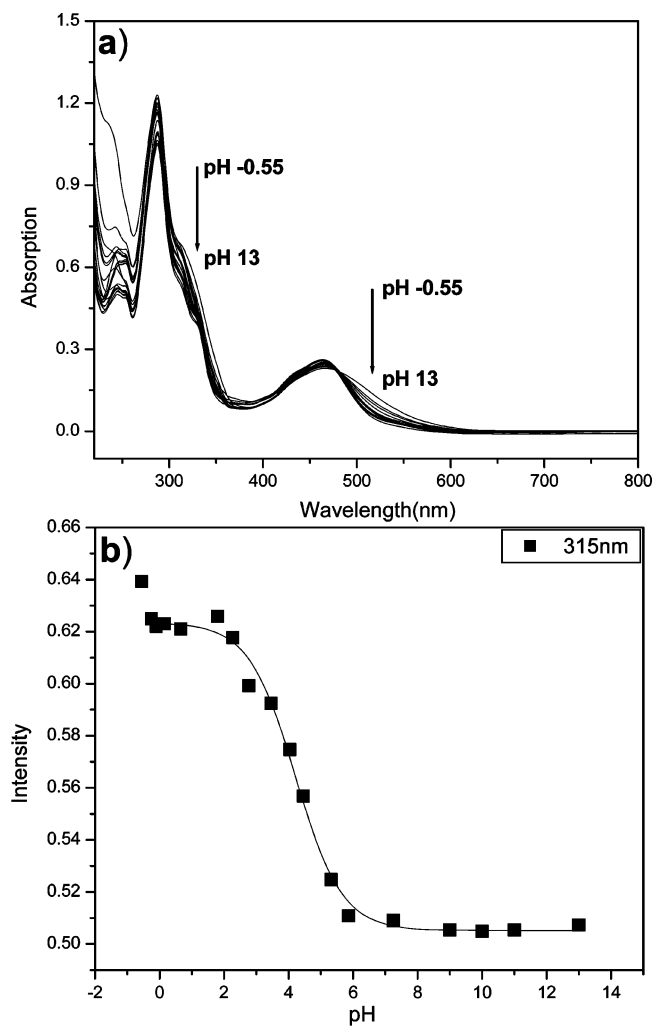


**Figure 2.** (a) Absorption spectra of  $[(bpy)_2RuL]^{2+}$  ( $2.0 \times 10^{-5}$  M) in aqueous solution as a function of pH ( $-0.55 \rightarrow 13$ ). (b) Plot of change in absorbance at 315 nm vs pH.

excited states due to the presence of protonable nitrogens on ligand L. Absorption spectra of  $[(bpy)_2RuL]^{2+}$  as a function of pH are shown in Figure 2a (pH changes accomplished by adding HCl or NaOH at an ionic strength of  $\sim 1.0$  M NaCl). The spectral changes were reversible with pH. The MLCT absorption consists of two bands at 426 and a shoulder at 464 nm. The high-energy band remains constant as a function of pH, whereas the low-energy band red-shifts to  $\sim 500$  nm as the pH is increased, which results in an overall broadening and flattening of the band (Figure 2a). A plot of the absorbance at  $\sim 315$  nm arising from ligand L versus pH shows an inflection point at  $pH \sim 4$  (Figure 2b), suggesting a  $pK_a \sim 4.0$  for monoprotonation of the parent compound.

The emission spectra as a function of pH (excitation wavelength 480 nm) are shown in Figure 3a. A plot of luminescence intensity at 675 nm versus pH shows two inflection points at  $pH \sim 2$  (sharp) and  $pH \sim 6$ . At pH 0 and lower, the luminescence intensity of the complex is negligible. The luminescence properties are reversible with pH. Stern–Volmer plots as a function of pH are shown in Figure 4 for two pH ranges of 4–10 and 0.55–4. The plot is linear only in the acidic pH range. ( $I_0$  values were taken at  $pH \sim 10$  and 3.8 for the plots covering the basic and acidic range, respectively).

### III.2. Photolysis of $[(bpy)_2RuL]^{2+}$ in Aqueous Solutions.

**III.2.a. Spectroscopic Changes.** The photochemistry of  $[(bpy)_2RuL]^{2+}$  upon irradiation by visible light in acetonitrile and aqueous

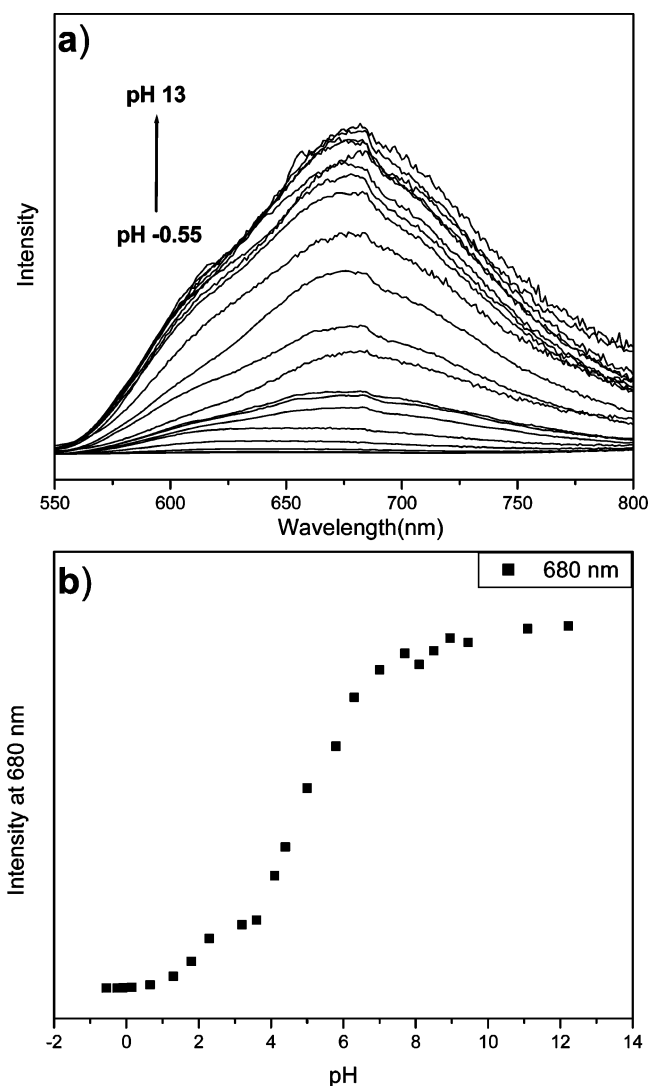


**Figure 3.** (a) pH dependence of the emission spectra for  $[(bpy)_2RuL]^{2+}$  ( $2.0 \times 10^{-5}$  M) in water (excitation wavelength is 480 nm). (b) Plot of emission intensity at 680 nm vs pH.

solutions was examined. In acetonitrile, no changes were observed in the absorption and emission spectra. In contrast, photolysis of  $[(bpy)_2RuL]^{2+}$  in aqueous solutions resulted in significant spectral changes. Figure 5a shows the absorption spectra of  $[(bpy)_2RuL]^{2+}$  as a function of irradiation time (7 h) in deionized water ( $pH \sim 7$ ). The 330 nm band diminishes with time, accompanied by an increase of the 254 nm band. Slight decreases in intensities of 284 and 464 nm were also observed. Changes were also observed in the emission spectra (Figure 5b). The emission maximum exhibited an  $\sim 55$  nm blue-shift, and the intensity of the band increased by an order of magnitude upon 7 h of photolysis. The spectral changes of  $[(bpy)_2RuL]^{2+}$  in aqueous solutions are observed even with room light exposure within a few hours. However, no spectral changes were observed if the solutions were maintained in the dark.

To explore the effect of pH on the photoreactivity of the complex, solutions at  $pH = 4$  (acetate buffer, 0.01 M),  $pH = 7$  (phosphate buffer, 0.01 M), and  $pH = 12$  (phosphate buffer, 0.01 M) were studied. The photochemistry was monitored by the change in intensity of  $\lambda_{max}$  of the emission peak. Figure 6 shows that the rate of photochemical reactions depend on the pH of the solution, with spectral changes occurring faster with increasing pH, but with no significant changes at  $pH = 4$  or  $pH < 4$  (data not shown).

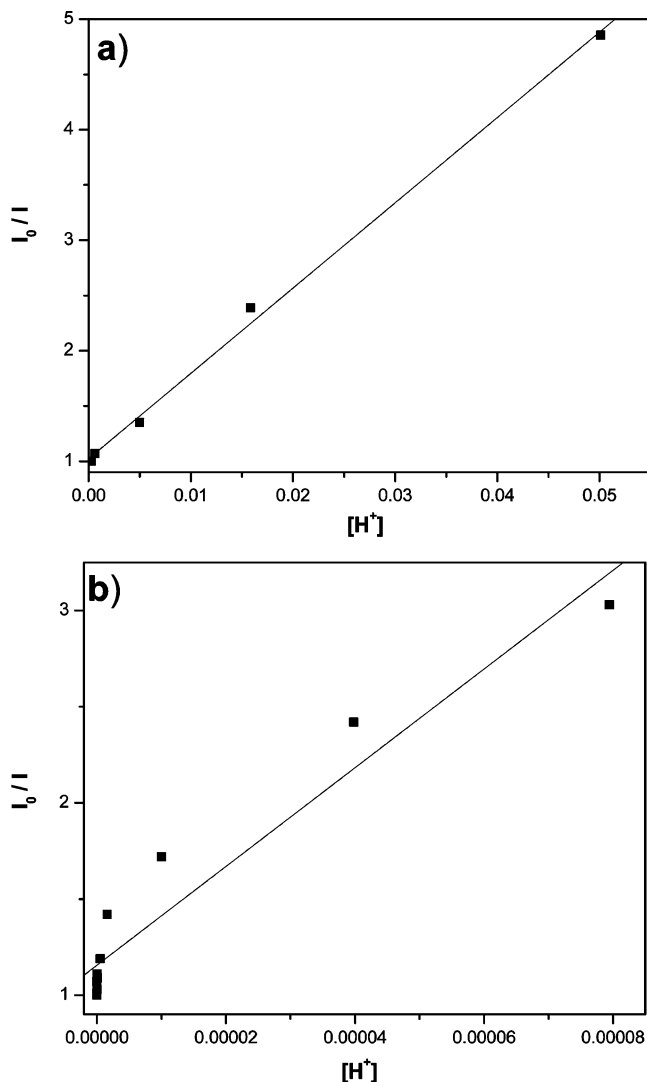


**Figure 4.** Stern–Volmer plots for the pH quenching of the luminescence of  $[(bpy)_2RuL]^{2+}$  ( $2.0 \times 10^{-5}$  M): (a)  $1 < \text{pH} < 4$ , slope = 77.2, intercept = 1.0, corresponding coefficient = 0.998; (b)  $4 < \text{pH} < 10$ ; slope =  $2.5 \times 10^4$ , intercept = 1.1, corresponding coefficient = 0.97.

Resonance Raman spectra of samples obtained before and after irradiation of aqueous  $[(bpy)_2RuL]^{2+} \cdot 2Cl^-$  for 8 h were recorded. After photolysis, the  $PF_6^-$  salt was generated and Raman spectra were recorded using  $CH_3CN$  as solvent, due to the stronger fluorescence background observed in water (concentration 1.0 mM). Figure 7 shows the Raman spectra obtained in resonance with the MLCT excitation. For  $[(bpy)_2RuL]^{2+}$  before irradiation, bands observed at 1171, 1216, 1332, 1427, 1541, and  $1639\text{ cm}^{-1}$  are assigned to vibrations from the L ligand.<sup>17</sup> The major change after irradiation is the loss of intensity of the band at  $1639\text{ cm}^{-1}$  assigned to the  $-C=C-$  stretch.

**III.2.b. Photolysis Products.** Components present in the starting solution of  $[(bpy)_2RuL]^{2+}$  as well as photoproducts formed after visible-light irradiation in aqueous solutions were analyzed by HPLC equipped with a photodiode array detector. For the unphotolyzed solution of  $[(bpy)_2RuL]^{2+}$ , chromatograms obtained by monitoring species at 450 nm show two peaks with a retention time of  $\sim 5.3$  min (peak A in Figure 8) and a minor component at  $\sim 3.9$  min (peak B). The absorption spectra of species related to each chromatographic peak are shown in Figure 9a. For species B, the band at 330 nm has lower intensity compared to species A (Figure 9a). The retention times,

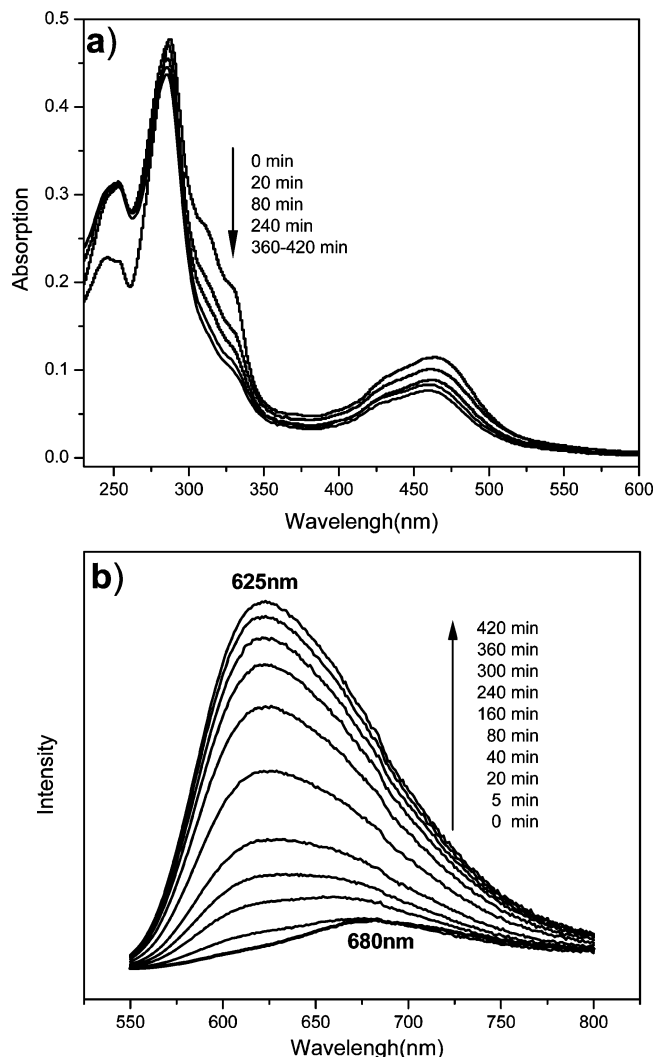


**Figure 5.** Visible-light irradiation of  $[(bpy)_2RuL]^{2+}$  ( $1.0 \times 10^{-5}$  M) in aqueous solution ( $\text{pH} = 7$ ) as a function of time: (a) absorption spectra; (b) emission spectra (excitation wavelength is 450 nm).

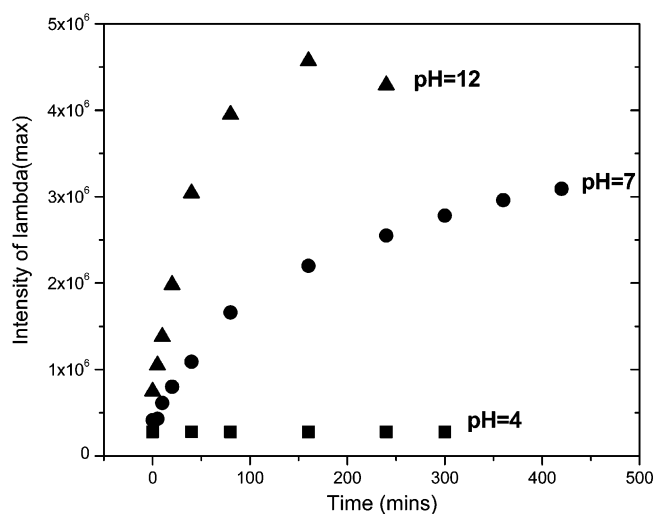


**Figure 6.** Intensity of emission maximum during visible-light irradiation of  $[(bpy)_2RuL]^{2+}$  ( $1.0 \times 10^{-5}$  M) at pH 4, 7, and 12.

spectroscopic properties, and  $m/z$  values obtained by LC–MS are presented in Table 1. LC–MS analysis of species present in fractions A and B produced doubly charged ion peaks centered at  $m/z = 389.1$  assignable to  $[(bpy)_2RuL]^{2+}$  (calcd 389.1 for  $[C_{44}H_{36}N_8Ru]^{2+}$ ). The LC–MS data is identical to

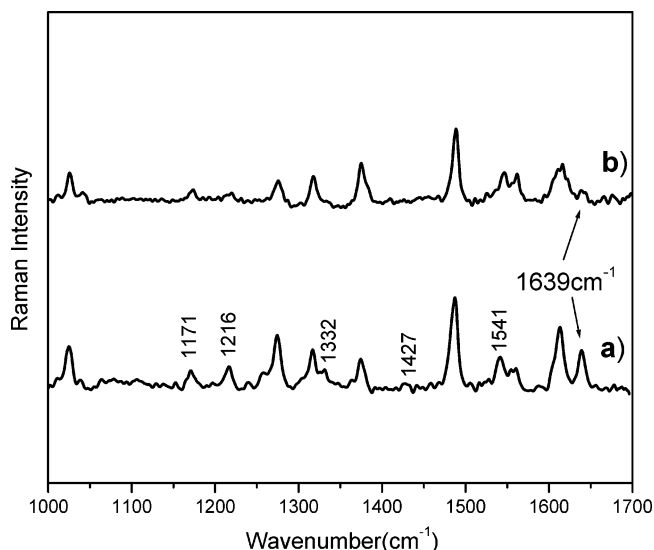


**Figure 7.** Resonance Raman spectra of  $[(bpy)_2RuL]^{2+} \cdot 2(PF_6^-)$  in  $CH_3CN$  with 488.0 nm excitation ( $1.0 \times 10^{-3}$  M) (a) before and (b) after light irradiation.

mass spectral data for as-synthesized  $[(bpy)_2RuL]^{2+}$  obtained by ESI-MS and shown in Figure 10a.

After 8 h of photolysis at neutral pH the HPLC trace (Figure 8b) shows that peak A has almost disappeared and peak B along with four new peaks C, D, E, and F are observed. The compound represented in F is the major product ( $\sim 90\%$ ) with a retention time of  $\sim 8.3$  min and C, D, and E are minor components (total amount  $< 5\%$ ) with shorter retention times. Peak B is of the order of 5%. The 330 nm band is completely lost in the species in peak F (Figure 9b). By use of semipreparative chromatography, the material in fraction F was isolated. The ESI-MS of fraction F contains a triply charged ion peak at  $m/z = 578.5$  and a doubly charged ion peak at 389.1, as shown in Figure 10b. The  $m/z$  578.5 peak is assigned to 1-heptanesulfonic ion-paired adduct of a dimer of  $[(bpy)_2RuL]^{2+}$  (calcd  $m/z$  578.5 for  $[C_{44}H_{36}N_8Ru^{2+}]_2 \cdot [C_7H_{15}SO_3^-]$ ). We suggest that the  $m/z$  389.1 peak arises from the monomer  $[(bpy)_2RuL]^{2+}$  (calcd  $m/z$  389.1) via fragmentation of the dimer during the MS measurement. Mass spectra obtained from an aqueous irradiated solution of  $[(bpy)_2RuL]^{2+}$  (in the absence of ion-pair reagent) also shows a triply charged ion peak at  $m/z$  561.11, assigned to  $[C_{44}H_{36}N_8Ru^{2+}]_2 \cdot I^-$  (calcd 561.11). The source of iodide is from sodium iodide added for electrospray ionization (MS shown in the Supporting Information).

Fractions C, D, and E could not be isolated by preparative chromatography due to the presence of small amounts of these compounds in a high concentration of ion-pair reagents. Peak C eluting with a short retention time of 1.4 min had absorption bands at 245, 288, and 458 nm (Figure 9b). The absorption spectrum of compound D which eluted with a retention time of 1.6 min is also shown in Figure 9b, with bands at 244, 292, 360, and 498 nm. Compound E eluting with a retention time of 2.1 min has bands at 242, 289, 350, and 484 nm (Figure 9b). The 330 nm band is absent in all these samples.

Since no degradation of  $[(bpy)_2RuL]^{2+}$  was noted at pH  $\sim 4$ , no analysis of the photoproducts was carried out. However, at pH  $> 12$ , the photodegradation was more pronounced than at pH 7, and HPLC of the photoproducts was carried out for a sample photolyzed at pH 13.3. As shown in Figure 11, after 2 h of photolysis, the starting material has disappeared. A major product peak is observed with a low retention time of 2 min; the absorption spectrum shows that the 330 nm band is absent.

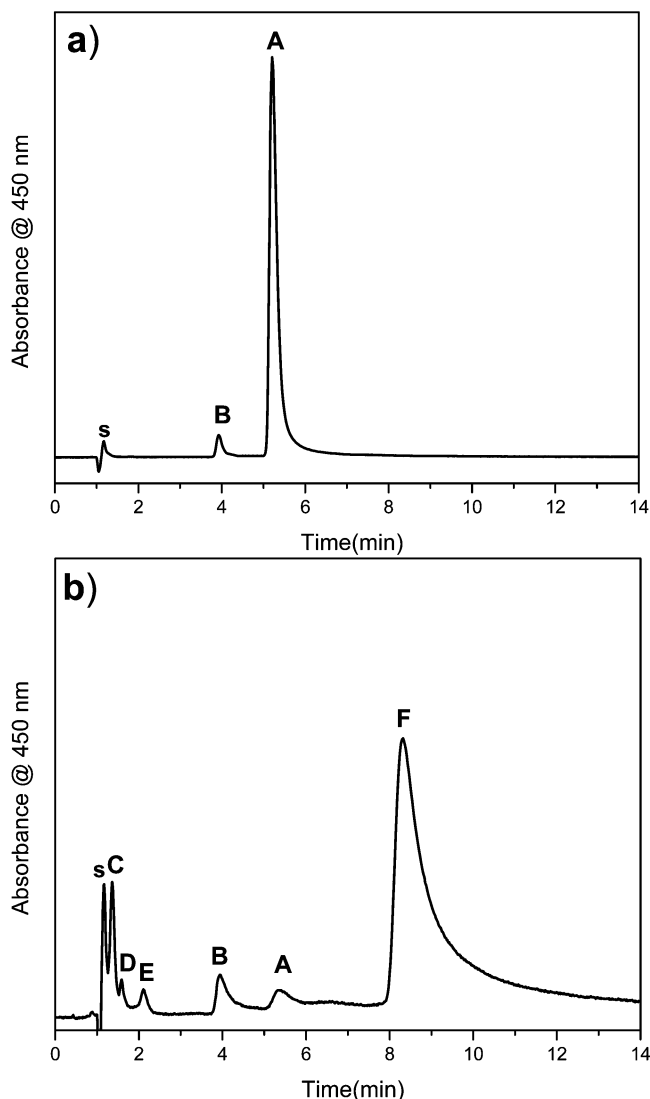


**Figure 8.** HPLC trace with detection at 450 nm of a solution of  $[(bpy)_2RuL]^{2+}$  ( $1.0 \times 10^{-3}$  M) (a) before and (b) after 8 h of photolysis in water (pH = 7).

We did not carry out detailed characterization of this photoproduct since the eventual application of  $[(bpy)_2RuL]^{2+}$  will be in neutral or acidic solutions. However, comparisons of Figures 8 and 11 clearly show that the photoproducts at pH  $\sim 7$  and  $\sim 13$  are distinct from each other, indicating different pathways of photochemical degradation.

#### IV. Discussion

The interest in ligand L was motivated by studies that polypyridyl complexes of Ru with L are attractive candidates as photosensitizers for artificial photosynthetic systems.<sup>17</sup> Such compounds are reported to have lifetimes in excess of microseconds and red-shifted emission bands, e.g.,  $[Ru(dmb)_2L]^{2+}$  in acetonitrile has emission  $\lambda_{max}$  of 732 nm and lifetime of 1150 ns as compared to  $[Ru(dmb)_3]^{2+}$  with a  $\lambda_{max}$  of 642 nm and lifetime of 950 ns (dmb = 4,4'-dimethyl-2,2'-bipyridine).<sup>17</sup> However, the emission quantum yields for complexes with the L ligand were lower by an order of magnitude. A detailed study has been carried out on a diruthenium species, coordinated via the free bipyridine part of the L ligand,  $[(dmb)_2Ru(L)Ru(dmb)_2]^{4+}$ . On the basis of various spectroscopic techniques, the electron in the excited state was proposed to be delocalized over the L ligand.<sup>17</sup> The binuclear Ru complex was found to

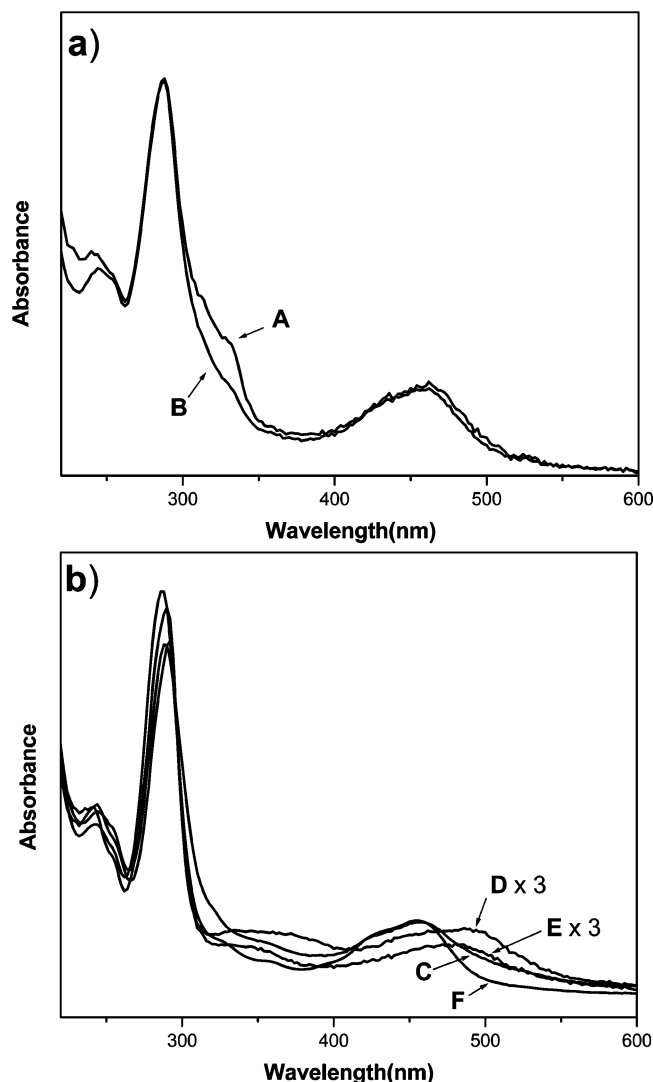


**Figure 9.** Absorption spectra of (a) peaks A and B and (b) peaks C–F corresponding to Figure 8.

be stable toward ligand loss upon irradiation in acetonitrile. No photolysis studies were reported in aqueous medium. Elliott and co-workers have examined a ligand which is a dimer of 4,4'-dimethyl-2,2'-bipyridine, in which *N,N'*-dialkylation of one end of the dimer leads to a diquat-modified ligand, the other end complexed to bis(bipyridine) ruthenium.<sup>7b,c</sup> These complexes without a double bond were photostable over a period of hours exposed to room light, but after several days, the emission was increased, indicating photodegradation.<sup>7b,c</sup> The photoproducts were not analyzed.

**IV.1. Acid–Base Chemistry of [(bpy)<sub>2</sub>RuL]<sup>2+</sup>.** The titration data of [(bpy)<sub>2</sub>RuL]<sup>2+</sup> shown in Figure 2a indicates that the p*K*<sub>a</sub> for monoprotonation is ~4, indicating that the bound ligand L is a weaker base than pyridine (p*K*<sub>a</sub> ~ 5.3). Also, evident in Figure 2a is the red-shifting of the 464 nm band with protonation indicating that conjugation extends over the entire ligand L, with the two bipyridyl moieties in electronic communication through the olefinic bond. The protonation-induced red-shifts are consistent with previous experimental<sup>37</sup> and theoretical studies<sup>38</sup> which showed MLCT bands exhibit red-shifts when nitrogen atoms on the ligand are protonated or coordinated to electron acceptors, e.g., BF<sub>3</sub>.

The emission titration data in Figure 3 provides information about excited-state acid–base chemistry. Studies have shown that in mixed-ligand Ru–polypyridyl complexes, the excited

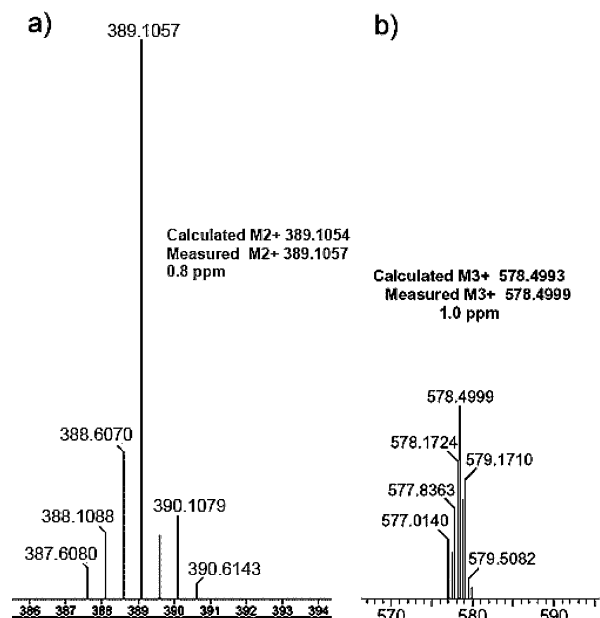


**Figure 10.** ESI-MS of (a) the starting compound [(bpy)<sub>2</sub>RuL]<sup>2+</sup> (A) and (b) 1-heptanesulfonic ion-paired adduct of a sample isolated from fraction F.

electron is localized on the most reducible ligand.<sup>17</sup> In cases where the electron-localized ligand is protonated, the formation of the MLCT state can cause significant changes in the excited-state acid–base chemistry.<sup>39</sup> Two apparent p*K*<sub>a</sub>\*'s are evident from the emission titration in Figure 3b, around 2 and 6.

The thermodynamic p*K*<sub>a</sub>\*'s of the excited state can be derived from the apparent p*K*<sub>a</sub>\*'s by two methods. If equilibrium is established between the protonated and deprotonated forms during the lifetime of the excited state, then the excited-state lifetimes of the deprotonated and protonated forms can be used to calculate p*K*<sub>a</sub>\*. A second method, based on the Forster cycle, uses the absorption energies of the acid and base, and a good estimate of the 0–0 transition energy is required. At pH 3.2, three lifetimes are observed. Two of these at 531 and 765 ns are assigned to τ<sub>LH</sub><sup>+</sup> and τ<sub>L</sub> for the lifetimes of mono and unprotonated [(bpy)<sub>2</sub>RuL]<sup>2+</sup> species. The third species with a lifetime of 109 ns could be arising from the minority component of the monoprotinated *cis* form. Using the lifetimes of 531 and 765 ns, the two excited-state p*K*<sub>a</sub>\*'s are calculated at 2.7 and 5.8. The Forster's cycle calculation requires the transition energy of the unprotonated and protonated forms for the triplet MLCT state.<sup>19,30</sup> Since this data is not available, we have not used this method.

The larger value of p*K*<sub>a</sub> for [(bpy)<sub>2</sub>RuL]<sup>2+</sup> in the excited state (2 units higher) compared to that in the ground state implies that the coordinated L is stronger base in the excited state. Increase in basicity of about ~5 pH units has been noted for the \*[Ru(bpy)<sub>2</sub>(dpp)]<sup>2+</sup> complex (dpp = 2,3-bis(2-pyridyl)pyrazine) due to electron delocalization on the dpp ligand in the excited state.<sup>29</sup> An even more extreme example is [Ru(bpy)<sub>2</sub>(bpz)]<sup>2+</sup> (bpz = 2,2'-bipyrazine), with p*K*<sub>a</sub> and p*K*<sub>a</sub>\* being –0.15 and +8.2, respectively.<sup>29</sup> The difference in p*K*<sub>a</sub> and p*K*<sub>a</sub>\* depends on the ability of the electron in the excited state to delocalize on the ligand. Examples are known where p*K*<sub>a</sub> and p*K*<sub>a</sub>\* values differ by only 0.4 units.<sup>31</sup>

**IV.2. Structural Identity of Photoproducts.** The HPLC of the starting material shown in Figure 8a has a major peak at A (~95%) and is assigned to [(bpy)<sub>2</sub>RuL]<sup>2+</sup>, based on the electronic and mass spectra. We also suggest that this compound is the *trans* form, in which the two “bpy” units in L are in *trans*

**TABLE 1: Retention Time, Spectral Properties, and  $m/z$  of the Chromatographic Peaks in Figure 8 and Proposed Structural Assignments**

peak	retention time (min)	$\lambda_{\max}$ (nm)	$m/z$	possible species
C	1.4	245, 288, 458		$[(bpy)_2Ru^{2+}(LH-OH)]$
D	1.6	244, 292, 360, 498		$trans-[(bpy)_2Ru^{2+}(H_2O)_2]$
E	2.1	242, 289, 350, 484		$cis-[(bpy)_2Ru^{2+}(H_2O)_2]$
B	3.9	244, 288, 330, 463	389.1	$cis-[(bpy)_2Ru^{2+}L]$
A	5.3	242, 288, 330, 463	389.1	$trans-[(bpy)_2Ru^{2+}L]$
F	8.3	243, 288, 458	389.1, 578.5	$[(bpy)_2Ru^{2+}L]_2[C_7H_{15}SO_3^-]$

configuration to each other. Since the more stable form of L is the trans isomer, it is reasonable to expect that  $[(bpy)_2RuL]^{2+}$  is primarily the trans form.<sup>17</sup> However, besides  $trans-[(bpy)_2RuL]^{2+}$  (peak A) in the HPLC, there is also a minor peak B, with the same mass spectral pattern as A, but a lower intensity absorption band at 330 nm (Figure 9a). We assign peak B to the cis isomer of  $[(bpy)_2RuL]^{2+}$ . The weaker interligand  $\pi-\pi^*$  transition arises from the distorted  $\pi$ -conjugation system due to the constrained structure in the cis configuration. This is consistent with previous studies which showed that transition metal complexes containing cis isomer of stilbazole,<sup>23</sup> 1,2-bis-(4-pyridyl)ethylene<sup>40</sup> and other stilbene-like ligands,<sup>27</sup> had weaker intraligand  $\pi-\pi^*$  transition bands compared to their trans isomers. Two lifetimes observed in acetonitrile at 710 and 256 ns are assigned to the trans and cis forms, respectively. It is unclear how the  $cis-[(bpy)_2RuL]^{2+}$  is forming. Ligand L was purified and  $trans-[(bpy)_2RuL]^{2+}$  isolated by chromatography. A possibility for the small amount of  $cis-[(bpy)_2RuL]^{2+}$  in the unirradiated sample can be due to photoreactions induced by room light during preparation and handling of the solutions.

Upon photolysis, the main product isolated (peak F) by preparative HPLC is the photodimer of the  $[(bpy)_2RuL]^{2+}$  complex. Mass spectra (Figure 10b) of F shows a triply charged ion peak at  $m/z$  578.49 attributed to the ion-paired adduct of the dimer (calculated value for  $[C_{95}H_{87}N_{16}Ru_2SO_3]^{3+}$ : 578.49). The complete disappearance of 330 nm band after irradiation indicates the loss of the olefin bond and the conjugation between the two bipyridine rings. The emission spectrum resembles  $[(bpy)_3Ru]^{2+}$  and also supports the loss of the double bond.

The absorption spectra of D and E (Figure 9) match that of trans and cis isomers of  $[Ru(bpy)_2(H_2O)]^{2+}$ , respectively.<sup>41,42</sup> Peak C is assigned to a photohydration OH adduct due to its

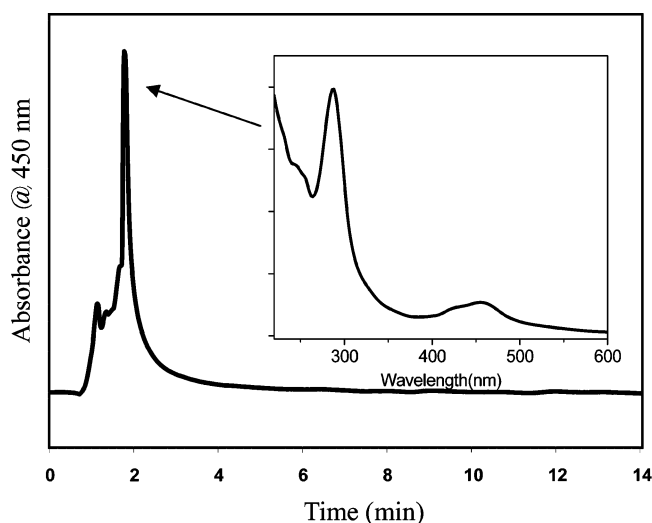


**Figure 11.** HPLC trace with detection at 450 nm of a solution of  $[(bpy)_2RuL]^{2+}$  ( $1.0 \times 10^{-3}$  M) after photolysis in pH 13.3 solution for 2 h (the inset shows the absorption spectrum of the major peak at 1.85 min).

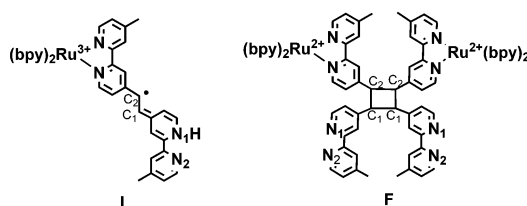
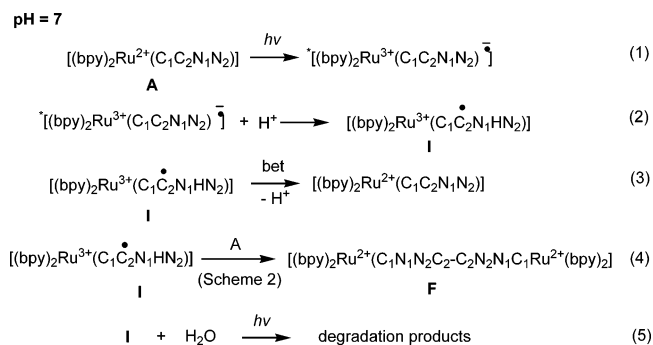
low retention time. For all these products, the absorption spectra show the lack of the 330 nm band.

**IV.3. Mechanisms of the Photochemical Reaction in Aqueous Solutions.** Spectroscopic and chromatographic data indicate formation of several products after visible-light irradiation of  $[(bpy)_2RuL]^{2+}$  in aqueous solutions at neutral and basic pHs, but no changes at acidic pH, and the discussion below focuses on these observations.

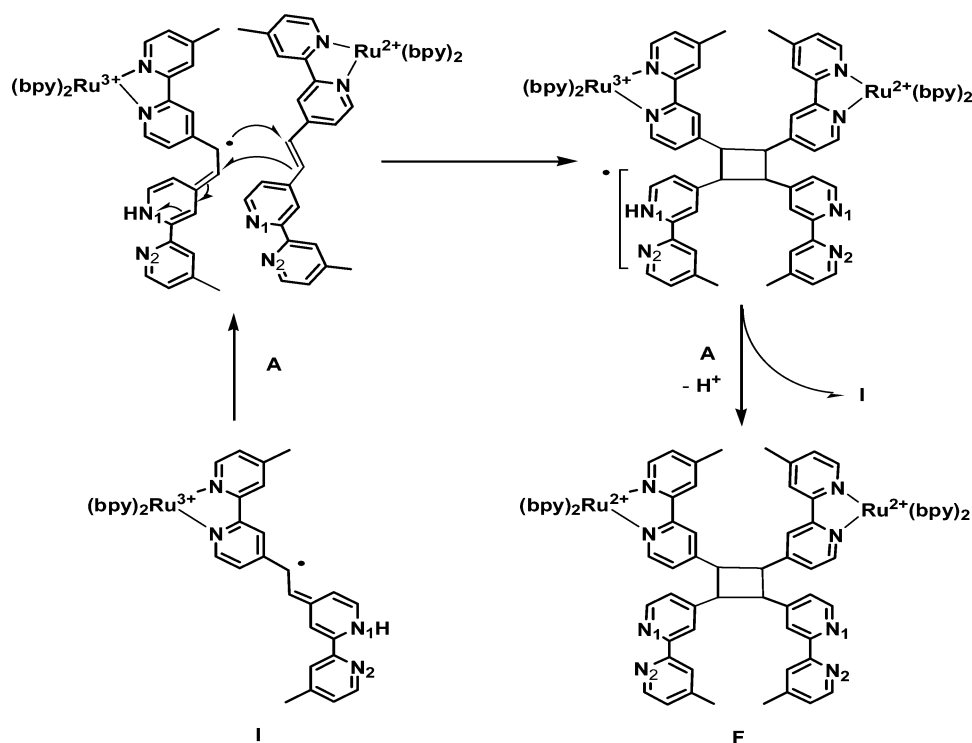
*IV.3.a. pH ~ 7.* Scheme 1 is the proposed mechanism in the neutral pH range. In reaction 1 the MLCT excitation leads to electron localization on the L ligand in the excited state.<sup>17,43</sup> Electrochemical studies have shown that L ligand is more easily reduced than bpy.<sup>43</sup> Transient absorption studies measured in acetonitrile confirm that L has a radical anion character.<sup>17</sup>

Reaction 2 represents the acid–base equilibrium in the excited state. The increase of the electron density on L ligand leads to an enhancement of basicity of in the excited state ( $pK_a^* \sim 6$ ). Addition of the proton is expected to occur at the position with highest electron density of radical anion, i.e., the nitrogen atoms. Quenching of the excited state by protonation has been observed for Ru polypyridyl complexes containing ligands with protonable sites.<sup>28,30,35</sup> The product I formed in reaction 2 as a result of protonation and electron localization is a radical with structure shown in Scheme 1 (I). The Stern–Volmer plot in Figure 4b indicates that emission quenching is indeed occurring with pH, but the nonlinear nature of the plot suggests that other reactions are also occurring. Inspection of Figure 3a shows a shoulder at 625 nm, and there could be formation of minor amounts of photoproducts that influence the emission data. In aprotic solvents, such as acetonitrile, no photoreaction was observed under visible-light irradiation, since intermediate A does not get protonated.

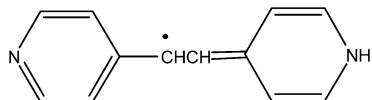
### SCHEME 1



## SCHEME 2



Several groups have studied the photochemistry of *trans*-1,2-bis(4-pyridyl)ethylene (BPE) in aqueous solutions.<sup>19–22</sup> In these studies, it was proposed that a radical intermediate (shown below) is involved in photoreactions. The formation of the radical intermediate is via hydrogen abstraction by nitrogen and subsequent rearrangement.<sup>19</sup> The ligand  $L$  has a similar structure as BPE and species  $I$  has a proposed structure similar to the radical intermediate shown below.



Photoaddition reactions of 1,2-bisbipyridyl ethylenes at the double bond were proposed to proceed through a radical intermediate localized on the C atom of the double bond which is stabilized by protonation of the pyridine nitrogen.<sup>22</sup> Pulse radiolysis and laser flash photolysis studies of *trans*-1,2-bis(4-pyridyl)ethylene ( $M$ ) in aqueous solution show that upon attachment of an electron to  $M$ , the product formed is  $MH^\cdot$ , with the electron localized on one of the ethylenic carbons, and protonation of the pyridyl nitrogen, similar to the structure proposed for  $I$  in Scheme 1.<sup>19</sup> The product formed upon quenching of photoexcited  $Ru(bpy)_3^{2+}$  by *N*-methyl-4-( $\beta$ -styryl)pyridinium halide leads to an intermediate with the electron delocalized over the *p*-styryl group.<sup>44</sup>

The presence of the cis isomer of  $[(bpy)_2RuL]^{2+}$  both in the initial material and upon photolysis can be understood based on the structure of  $I$ . Since the bond order of the olefin decreases in  $I$ , there is possibility for rotation around the C–C bridge bond. In the case of  $[Ru(bpy)_2L_n]^{m+}$  complexes with  $L$  being 4-stilbazole ( $n = 1, 2$ ), irradiation of the MLCT band leads to photostationary states with primarily the *trans* isomer and minor amounts of the *cis* isomer of the coordinated 4-stilbazole ligand. The excited state was described as oxidized metal-radical anion 4-stilbazole ligand.<sup>23</sup> In fact, *cis*–*trans* isomerization of stilbene-like ligands has been reported to occur via a radical intermediate

induced by electron transfer (ET) from excited sensitizers.<sup>44–47</sup> These studies suggested a radical-type intermediate was produced, which has a single-bond character.<sup>48</sup> In all reported cases with the involvement of a radical intermediate, *trans* isomer was found to be the dominant product.

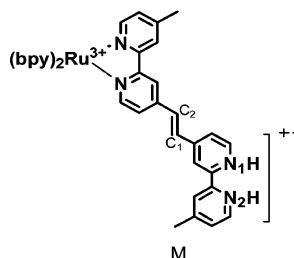
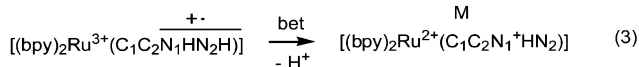
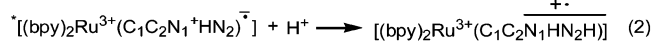
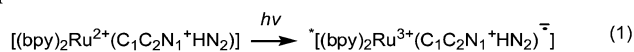
Reaction 3 represents deprotonation followed by back ET to generate  $[(bpy)_2RuL]^{2+}$ . Reaction 4 describes the reaction of  $I$  with the parent compound to form the dimeric product  $F$ , as shown in Scheme 2. It may be unexpected that dimerization will occur since a low concentration of the monomer was used ( $<10^{-5}$  M). A previous study on the photolysis of the methiodide salt of 4-stilbazole salt noted that the dimer of the salt was the major product.<sup>21</sup> It was proposed that given a long organic entity with a charge at one end, aggregates might be expected to be formed in the aqueous solution, and thus dimerization might result from reactions occurring within these aggregates, though the exact mechanism was not examined.<sup>21</sup> The mass spectral data of  $F$  is consistent with a dimer containing a cyclobutane ring. Studies of styrene radical cations (terminal olefin) and anethole (internal olefin) have shown that the dimerization can occur via the  $[2 + 1]$  cycloaddition reactions of the cation radical with a neutral molecule via a concerted reaction.<sup>49,50</sup> In the case of stilbene, dimerization is also observed, but to a  $\pi$  and  $\sigma$  complex, and the cyclobutane ring formation has not been reported, since the higher temperature stable  $\sigma$  complex dissociates to the monomer radical cation and the parent compound, instead of forming the cyclobutane ring.<sup>51</sup> We are unsure of the exact mechanism for formation of  $F$ , but on the basis of the previous olefin radical cation promoted dimerization propose Scheme 2. The cycloaddition reaction followed by deprotonation and internal ET to the Ru(III) will result in the observed photoproduct,  $F$ .

Besides  $F$ , several other species were also found in the HPLC. These include an OH adduct based on its shorter retention time and absorption spectrum. The shortening of retention time is due to the increased polarity caused by the hydroxyl group.<sup>52</sup> Products  $D$  and  $E$  are assigned to *trans* and *cis* isomers of  $[Ru$



## SCHEME 3

pH ≤ 4



$(\text{bpy})_2(\text{H}_2\text{O})]^{2+}$ . The disappearance of the 330 nm band due to the olefinic group is also in accord with the structure of these products. Reaction 5 in Scheme 1 describes the photolytically driven degradation of I (containing Ru(III)) to form these products. The thermal and photochemical reduction of Ru( $\text{bpy}$ ) $_3^{3+}$  with water has been studied.<sup>52,53</sup> This chemistry is very complex, with about 10% of the complex being converted to a number (~10) of Ru-containing species and the rest as Ru( $\text{bpy}$ ) $_3^{2+}$ . Degradation of the bpy ligand as well as CO $_2$  formation was observed. In the dark, the rate of Ru( $\text{bpy}$ ) $_3^{3+}$  reduction increases dramatically with pH. Upon illumination with visible light, the rate of disappearance of Ru( $\text{bpy}$ ) $_3^{3+}$  is increased, with similar end products as in the thermal reaction. The reaction of photoexcited  $^*\text{Ru}(\text{bpy})_3^{3+}$  with water is reported to be extremely rapid, 10 $^9$  times more rapid than the ground-state reaction with OH $^-$  (basic solutions).<sup>52</sup>

*IV.3.b. pH ≤ 4.* At pH 4 or below, there were no spectral changes upon photolysis of  $[(\text{bpy})_2\text{RuL}]^{2+}$ , indicating that no photoproducts were forming. The proposed reactions involved in the photochemistry of  $[(\text{bpy})_2\text{RuL}]^{2+}$  at pH < 4 are shown in Scheme 3. The Stern–Volmer plots for pH 0–4 (Figure 4a) indicate that emission quenching of the excited state occurs by reaction with protons. The bimolecular quenching rate constant was found to be  $1.4 \times 10^8 \text{ M}^{-1} \text{ s}^{-1}$  ( $K_{\text{SV}} = 74.6$ ,  $\tau_{\text{LH}}^+ = 531$  ns), indicating an activated process.<sup>31</sup> Below pH 4, the ground-state species is  $\{\text{RuN}_1\text{H}^+\text{N}_2\}$ , which in the excited state can be protonated at N $_2$ . With protonation of the bipyridyl ligand, rapid quenching of the excited state can take place by intramolecular ET to the protonated pyridine ring (reaction 2 in Scheme 3). Such a quenching scheme was first reported for  $[(\text{bpy})_2\text{RuAB}]^{2+}$ , where AB is a bis-chelating 2,2':3',2'':6'',2'' quaterpyridine, composed of a bpy fragment A coordinated to Ru and a free bpy fragment B.<sup>31</sup> Below pH 1.5, proton quenching of the luminescence of  $[(\text{bpy})_2\text{Ru(III)ABH}^+]^{3+}$  via second protonation of the BH fragment was proposed. For a related complex  $[(\text{bpy})_2\text{Ru(III)ABMe}]^{3+}$  (one of the N in the B fragment is quaternized with a CH $_3$  group), excited-state quenching by protonation of B was proposed.<sup>31</sup> Both the  $[\text{ABH}_2^{2+}]$  and  $[\text{BH}^+\text{MeH}^+]$  unit resemble a viologen-like electron acceptor. It was proposed that protonation led to the formation of a charge-separated  $[(\text{bpy})_2\text{RuABMeH}^+]^{4+}$ , with the  $[\text{BMeH}_2^{2+}]$  unit resembling the viologen-like unit acting as the electron acceptor. Transient spectroscopic studies did not detect the viologen-radical species.<sup>31</sup>

*IV.3.c. pH > 12.* Protonation of L is not expected in the excited state at pH ~ 13.3, with a  $\text{p}K_{\text{a}}^*$  of ~6. Thus, the proton-

coupled electron-transfer quenching shown in Scheme 1 is not expected and formation of a Ru(III) intermediate is unlikely. The photodecomposition leads to a very different HPLC profile at pH 13 as compared to pH 7 (Figure 11), suggesting a different pathway of photochemical decomposition at very basic pH. The UV–vis spectrum of the major product observed in HPLC indicates that the double bond in L is no longer present. We have not explored further the mechanism of degradation at basic pH since the application of these photosensitizers is expected in neutral or acidic solutions.

## V. Conclusions

Significant changes of absorption and emission spectral characteristics of  $[(\text{bpy})_2\text{RuL}]^{2+}$  in aqueous solutions under visible-light irradiation were observed. The photoreactions exhibited a pH dependence with no reaction below pH 4 and increasing spectroscopic changes under more basic conditions. With the use of spectroscopic, chromatographic, and mass spectrometric methods, products from photoreaction at neutral pH were isolated, with the major product identified as the dimer of  $[(\text{bpy})_2\text{RuL}]^{2+}$ . The mechanism proposed involves a radical intermediate formed via protonation in the excited state and electron localization on the double bond and explains the observed solvent and pH effects, the spectroscopic data, and pathways to observed products. Below pH 4, no photodegradation of  $[(\text{bpy})_2\text{RuL}]^{2+}$  was observed and emission quenching occurred by an internal ET to a viologen-type moiety formed upon excited-state protonation.

**Acknowledgment.** We acknowledge NASA and DOE Basic Energy Sciences for supporting this research. We also thank Dr. John Kuhn and Mr. Matt Woods at the Department of Chemical and Biomolecular Engineering for letting us use the Raman spectrometer.

**Supporting Information Available:** ESI-MS of  $[(\text{bpy})_2\text{RuL}]^{2+}$  after photolysis for 8 h in water (Figure S1). This material is available free of charge via the Internet at <http://pubs.acs.org>.

## References and Notes

- (1) Kalyanasundaram, K. *Coord. Chem. Rev.* **1982**, *46*, 159–244.
- (2) Lin, C.; Sutin, N. *J. Am. Chem. Soc.* **1975**, *97*, 3543–3545.
- (3) Sutin, N.; Creutz, C. *Pure Appl. Chem.* **1980**, *52*, 2717–2738.
- (4) Meyer, T. J. *Acc. Chem. Res.* **1978**, *11*, 94–100.
- (5) Huynh, M. H. V.; Dattelbaum, D. M.; Meyer, T. J. *Coord. Chem. Rev.* **2005**, *249*, 457–483.
- (6) (a) Calvert, J. M.; Caspar, J. V.; Binstead, R. A.; Westmoreland, T. D.; Meyer, T. J. *J. Am. Chem. Soc.* **1982**, *104*, 6620–6627. (b) Olmsted, J.; McClanahan, S. F.; Danielson, E.; Younathan, J. N.; Meyer, T. J. *J. Am. Chem. Soc.* **1987**, *109*, 3297–3301. (c) Boyde, S.; Strouse, G. F.; Jones, W. E.; Meyer, T. J. *J. Am. Chem. Soc.* **1989**, *111*, 7448–7454. (d) Baxter, S. M.; Jones, W. E.; Danielson, E.; Worl, L.; Strouse, G.; Younathan, J.; Meyer, T. J. *Coord. Chem. Rev.* **1991**, *111*, 47–71. (e) Mecklenburg, S. L.; Peek, B. M.; Erickson, B. W.; Meyer, T. J. *J. Am. Chem. Soc.* **1991**, *113*, 8540–8542. (f) Bignozzi, C. A.; Argazzi, R.; Garcia, C. G.; Scandola, F.; Schoonover, J. R.; Meyer, T. J. *J. Am. Chem. Soc.* **1992**, *114*, 8727–8729. (g) Jones, W. E.; Chen, P.; Meyer, T. J. *J. Am. Chem. Soc.* **1992**, *114*, 387–388. (h) Jones, W. E.; Baxter, S. M.; Strouse, G. F.; Meyer, T. J. *J. Am. Chem. Soc.* **1993**, *115*, 7363–7373. (i) Stavrev, K. K.; Zerner, M. C.; Meyer, T. J. *J. Am. Chem. Soc.* **1995**, *117*, 8684–8685. (j) Brennaman, M. K.; Alstrum-Acevedo, J. H.; Fleming, C. N.; Jang, P.; Meyer, T. J.; Papanikolas, J. M. *J. Am. Chem. Soc.* **2002**, *124*, 15094–15098. (k) Sykora, M.; Petruska, M. A.; Alstrum-Acevedo, J.; Bezel, I.; Meyer, T. J.; Klimov, V. I. *J. Am. Chem. Soc.* **2006**, *128*, 9984–9985. (l) Concepcion, J. J.; Brennaman, M. K.; Deyton, J. R.; Lebedeva, N. V.; Forbes, M. D. E.; Papanikolas, J. M.; Meyer, T. J. *J. Am. Chem. Soc.* **2007**, *129*, 6968–6969.
- (7) (a) Elliott, C. M.; Freitag, R. A. *Chem. Commun.* **1985**, 156–157. (b) Elliott, C. M.; Freitag, R. A.; Blaney, D. D. *J. Am. Chem. Soc.* **1985**, *107*, 4647–4655. (c) Cooley, L. F.; Headford, C. E. L.; Elliott, C. M.; Kelley, D. F. *J. Am. Chem. Soc.* **1988**, *110*, 6673–6682. (d) Ryu, C. K.; Wang, R.; Schmehl, R. H.; Ferrere, S.; Ludwikow, M.; Merkert, J. W.;

- Headford, C. E. L.; Elliott, C. M. *J. Am. Chem. Soc.* **1992**, *114*, 430–438.
- (c) Weber, J. M.; Rawls, M. T.; MacKenzie, V. J.; Limoges, B. R.; Elliott, C. M. *J. Am. Chem. Soc.* **2007**, *129*, 313–320.
- (8) (a) Krueger, J. S.; Mayer, J. E.; Mallouk, T. E. *J. Am. Chem. Soc.* **1988**, *110*, 8232–8234. (b) Kim, Y. I.; Mallouk, T. E. *J. Phys. Chem.* **1992**, *96*, 2879–2885. (c) Brigham, E. S.; Snowden, P. T.; Kim, Y. I.; Mallouk, T. E. *J. Phys. Chem.* **1993**, *97*, 8650–8655. (d) Yonemoto, E. H.; Riley, R. L.; Kim, Y. I.; Atherton, S. J.; Schmehl, R. H.; Mallouk, T. E. *J. Am. Chem. Soc.* **1993**, *115*, 5348–5348. (e) Yonemoto, E. H.; Kim, Y. I.; Schmehl, R. H.; Wallin, J. O.; Shoulders, B. A.; Richardson, B. R.; Haw, J. F.; Mallouk, T. E. *J. Am. Chem. Soc.* **1994**, *116*, 10557–10563. (f) Yonemoto, E. H.; Saupe, G. B.; Schmehl, R. H.; Hubig, S. M.; Riley, R. L.; Iverson, B. L.; Mallouk, T. E. *J. Am. Chem. Soc.* **1994**, *116*, 4786–4795.
- (9) (a) Dutta, P. K.; Incavo, J. A. *J. Phys. Chem.* **1987**, *91*, 4443–4446. (b) Dutta, P. K.; Turbeville, W. *J. Phys. Chem.* **1992**, *96*, 9410–9416. (c) Borja, M.; Dutta, P. K. *Nature (London)* **1993**, *362*, 43–45. (d) Dutta, P. K.; Ledney, M. *Prog. Inorg. Chem.* **1997**, *44*, 209–271. (e) Castagnola, N. B.; Dutta, P. K. *J. Phys. Chem. B* **1998**, *102*, 1696–1702. (f) Vitale, M.; Castagnola, N. B.; Ortins, N. J.; Brooke, J. A.; Vaidyalingam, A.; Dutta, P. K. *J. Phys. Chem. B* **1999**, *103*, 2408–2416. (g) Lee, H.; Dutta, P. K. *J. Phys. Chem. B* **2002**, *106*, 11898–11904. (h) Kim, Y.; Lee, H.; Dutta, P. K.; Das, A. *Inorg. Chem.* **2003**, *42*, 4215–4222. (i) Kim, Y.; Das, A.; Zhang, H.; Dutta, P. K. *J. Phys. Chem. B* **2005**, *109*, 6929–6932.
- (10) Sykora, M.; Kincaid, J. R. *Nature (London)* **1997**, *387*, 162–164.
- (11) Yi, X. Y.; Wu, L. Z.; Tung, C. H. *J. Phys. Chem. B* **2000**, *104*, 9468–9474.
- (12) Demas, J. N.; DeGraff, B. A. *Coord. Chem. Rev.* **2001**, *211*, 317–351.
- (13) Creutz, C.; Sutin, N. *Proc. Natl. Acad. Sci. U.S.A.* **1975**, *72*, 2858–2862.
- (14) Balzani, V.; Bergamini, G.; Marchioni, F.; Ceroni, P. *Coord. Chem. Rev.* **2006**, *250*, 1254–1266.
- (15) Polo, A. S.; Itokazu, M. K.; Murakami Iha, N. Y. *Coord. Chem. Rev.* **2004**, *248*, 1343–1361.
- (16) Juris, A.; Balzani, V.; Barigelletti, F.; Campagna, S.; Belsler, P.; von Zelewsky, A. *Coord. Chem. Rev.* **1988**, *84*, 85–277.
- (17) Strouse, G. F.; Schoonover, J. R.; Duesing, R.; Boyde, S.; Jones, W. E. J.; Meyer, T. J. *Inorg. Chem.* **1995**, *34*, 473–487.
- (18) Whitten, D. G.; McCall, M. T. *J. Am. Chem. Soc.* **1969**, *91*, 5097–5103.
- (19) Goerner, H.; Koltzenburg, G.; Schulte-Frohlinde, D. *J. Phys. Chem.* **1991**, *95*, 3993–3999.
- (20) Goerner, H.; Elisei, F.; Mazzucato, U. *J. Phys. Chem.* **1991**, *95*, 4000–4005.
- (21) Happ, J. W.; McCall, M. T.; Whitten, D. G. *J. Am. Chem. Soc.* **1971**, *93*, 5496–5501.
- (22) Whitten, D. G.; Lee, Y. J. *J. Am. Chem. Soc.* **1972**, *94*, 9142–9148.
- (23) Zarnegar, P. P.; Bock, C. R.; Whitten, D. *J. Am. Chem. Soc.* **1973**, *95*, 4367–4372.
- (24) Boyde, S.; Strouse, G. F.; Jones, W. E.; Meyer, T. J. *J. Am. Chem. Soc.* **1990**, *112*, 7395–7396.
- (25) Shaw, J. R.; Webb, R. T.; Schmehl, R. H. *J. Am. Chem. Soc.* **1990**, *112*, 1117–1123.
- (26) Litke, S. V.; Mezentseva, T. V.; Lyalin, G. N.; Ershov, A. Y. *Opt. Spectrosc.* **2003**, *95*, 917–924.
- (27) Polo, A. S.; Itokazu, M. K.; Frin, K. M.; de Toledo Patrocinio Antonio, O.; Murakami Iha, N. Y. *Coord. Chem. Rev.* **2006**, *250*, 1669–1680.
- (28) Hosek, W.; Tysoe, S. A.; Gafney, H. D.; Baker, A. D.; Streckas, T. C. *Inorg. Chem.* **1989**, *28*, 1228–1231.
- (29) Nazeeruddin, M. K.; Kalyanasundaram, K. *Inorg. Chem.* **1989**, *28*, 4251–4259.
- (30) Sun, H.; Hoffman, M. Z. *J. Phys. Chem.* **1993**, *97*, 5014–5018.
- (31) Guardigli, M.; Flamigni, L.; Barigelletti, F.; Richards, C. S. W.; Ward, M. D. *J. Phys. Chem.* **1996**, *100*, 10620–10628.
- (32) Casalbani, F.; Mulazzani, Q. G.; Clark, C. D.; Hoffman, M. Z.; Orizondo, P. L.; Perkovic, M. W.; Rillema, D. P. *Inorg. Chem.* **1997**, *36*, 2252–2257.
- (33) Liu, F.; Wang, K.; Bai, G.; Zhang, Y.; Gao, L. *Inorg. Chem.* **2004**, *43*, 1799–1806.
- (34) Hicks, C.; Ye, G.; Levi, C.; Gonzales, M.; Rutenburg, I.; Fan, J.; Helmy, R.; Kassis, A.; Gafney, H. D. *Coord. Chem. Rev.* **2001**, *211*, 207–222.
- (35) Encinas, S.; Morales, A. F.; Barigelletti, F.; Barthram, A. M.; White, C. M.; Couchman, S. M.; Jeffery, J. C.; Ward, M. D.; Grills, D. C.; George, M. W. *J. Chem. Soc., Dalton Trans.* **2001**, 3312–3319.
- (36) Valenty, S. J.; Behnken, P. E. *Anal. Chem.* **1978**, *50*, 834–837.
- (37) Thompson, A. M. W. C.; Smailes, M. C. C.; Jeffery, J. C.; Ward, M. D. *J. Chem. Soc., Dalton Trans.* **1997**, 737–743.
- (38) Bruschi, M.; Fantucci, P.; Pizzotti, M. *J. Phys. Chem. A* **2005**, *109*, 9637–9645.
- (39) Ireland, J. F.; Wyatt, A. H. *Adv. Phys. Org. Chem.* **1976**, *12*, 131–221.
- (40) Dattelbaum, D. M.; Itokazu, M. K.; Murakami Iha, N. Y.; Meyer, T. J. *J. Phys. Chem. A* **2003**, *107*, 4092–4095.
- (41) Durham, B.; Wilson, S. R.; Hodgson, D. J.; Meyer, T. J. *J. Am. Chem. Soc.* **1980**, *102*, 600–607.
- (42) Vaidyalingam, A.; Dutta, P. K. *Anal. Chem.* **2000**, *72*, 5219–5224.
- (43) Rajesh, C. S.; Zhang, H.; Dutta, P. K. To be submitted for publication.
- (44) Takagi, K.; Aoshima, K.; Sawaki, Y.; Iwamura, H. *J. Am. Chem. Soc.* **1985**, *107*, 47–52.
- (45) Takagi, K.; Ogata, Y. *J. Org. Chem.* **1982**, *47*, 1409–1412.
- (46) Happ, J. W.; Ferguson, J. A.; Whitten, D. G. *J. Org. Chem.* **1972**, *37*, 1485–1491.
- (47) Juskowiak, B.; Dominiak, A.; Takenaka, S.; Takagi, M. *Photochem. Photobiol.* **2001**, *74*, 391–400.
- (48) Fischer, G.; Muszkat, K. A.; Fischer, E. *J. Chem. Soc. B* **1968**, 1156–1158.
- (49) Lewis, F. D.; Kojima, M. *J. Am. Chem. Soc.* **1988**, *110*, 8664–8670.
- (50) Johnston, L. J.; Schepp, N. P. *Pure Appl. Chem.* **1995**, *67*, 71–78.
- (51) Majima, T.; Tojo, S.; Ishida, A.; Takamuku, S. *J. Phys. Chem.* **1996**, *100*, 13615–13623.
- (52) Ghosh, P. K.; Brunshwig, B. S.; Chou, M.; Creutz, C.; Sutin, N. *J. Am. Chem. Soc.* **1984**, *106*, 4772–4783.
- (53) Ledney, M.; Dutta, P. K. *J. Am. Chem. Soc.* **1995**, *117*, 7687–7695.